Scaling of fluctuations in one-dimensional interface and hopping models

P.-M. Binder,[1] M. Paczuski,[2] and Mustansir Barma[3,4]

[1] *Wolfson College, Oxford OX2 6UD, United Kingdom*

[2] *Department of Physics, Brookhaven National Laboratory, Upton, New York 11973*

[3] *Tata Institute of Fundamental Research, Homi Bhabha Road, Bombay 400 005, India**

[4] *Department of Physics, Theoretical Physics, 1 Keble Road, Oxford OX1 3NP, United Kingdom*

(Received 13 September 1993)

We study time-dependent correlation functions in a family of one-dimensional biased stochastic lattice-gas models in which particles can move up to k lattice spacings. In terms of equivalent interface models, the family interpolates between the low-noise Ising ($k = 1$) and Toom ($k = \infty$) interfaces on a square lattice. Since the continuum description of density (or height) fluctuations in these models involves at most $(k + 1)$th-order terms in a gradient expansion, we can test specific renormalization-group predictions using Monte Carlo methods to probe scaling behavior. In particular we confirm the existence of multiplicative logarithms in the temporal behavior of mean-squared height fluctuations [$\sim t^{1/2}(\ln t)^{1/4}$], induced by a marginal cubic gradient term. Analogs of redundant operators, familiar in the context of equilibrium systems, also appear to occur in these nonequilibrium systems.

PACS number(s): 05.40.+j, 02.50.Ey, 05.70.Ln, 68.35.−p

I. INTRODUCTION

Nonlinearities strongly affect the dynamics of systems out of equilibrium, and, in particular, influence scaling behaviors at large length and time scales. Progress in describing the effects of nonlinearities has been achieved by studying stochastic dynamical models [1]—both microscopic models of interfaces and lattice gases with probabilities assigned to various local moves, and continuum hydrodynamic models, where the probabilistic element enters through random noise. In this paper we address this issue by studying a new family of discrete stochastic models, and their coarse-grained continuum equivalents. These models have well-characterized nonlinearities, which make them very useful for carrying out a detailed examination of several renormalization-group (RG) predictions and issues such as marginality-induced logarithmic corrections to power laws, the dynamic equivalents of redundant operators, and the generation of relevant nonlinearities from higher-order nominally irrelevant ones.

The stochastic continuum equation [2, 3]

$$\frac{\partial h}{\partial t} = \nu \frac{\partial^2 h}{\partial x^2} + \sum_m b_m \left(\frac{\partial h}{\partial x} \right)^m + \eta(x,t) \qquad (1)$$

has played a key role in the theoretical developments. This equation describes the temporal evolution of a growing one-dimensional interface that obeys local dynamical rules. The quantity $h(x,t)$ is the local height, ν is the surface tension, and $\eta(x,t)$ is the noise term, which is taken to satisfy the white noise condition $\langle \eta(x,t)\eta(x',t') \rangle = D\delta(x - x')\delta(t - t')$. Alternatively, the equation can be viewed [4] as a noisy Burgers equation which describes the formation and dissipation of shock waves in a fluid system, with ν being the viscosity and $\partial h/\partial x$ being identified with density fluctuations. The scaling properties of height fluctuations

$$S^2(x,t) \equiv \langle [h(x + x', t) - h(x', 0)]^2 \rangle$$

depend on the coefficients b_m in the gradient expansion in (1). Generic behaviors, obtained from RG methods and mode coupling, are discussed in detail in Sec. 3. Three distinct growth laws are predicted. If all b_m coefficients vanish, $S(0,t) \sim t^{1/4}$ [5, 6]; if $b_0 = 0$ but $b_1 \neq 0$, the growth law is $S(0,t) \sim t^{1/2}$ [7]; while if b_0 and b_1 vanish but b_2 is nonzero, $S(0,t) \sim t^{1/3}$ [2, 3]. Any nonzero even-ordered coefficient b_m breaks the $h \to -h$ symmetry in this equation and gives rise to $t^{1/3}$ behavior even if the leading coefficient b_2 itself is zero. The physical meaning of the b_m coefficients and the conditions under which they vanish will be described later.

These scaling laws have been found to hold asymptotically for several discrete stochastic models of interfaces. Two previously studied models are particularly relevant here as they provide limits for the family of models that we introduce and study in this paper. The first describes a moving interface between up and down phases of a square lattice Glauber-Ising model in an external magnetic field [8, 9]; in the limit of large-exchange coupling, this reduces to the single-step ($k = 1$) model [10]. The second model pertains to an interface in the two-dimensional Toom model [11–13] in the low-noise limit. The infinite family of models for positive integer k interpolates between the two limits, and has the attractive feature that the continuum hydrodynamic description of the kth model has at most $k + 1$ nonzero b_m coefficients. This makes possible a systematic verification of the effects of successive nonlinearities.

Our study has the general objective of describing asymptotic growth laws and their basins of attraction. In particular, we test a recent prediction that if only odd-order b_m coefficients are present, then the $t^{1/4}$ growth law is modified to $t^{1/4}(\ln t)^{1/8}$ [14]. We also investigate long-time crossovers between different growth laws along special loci in the parameter space (see Secs. III and

*Permanent address.

IV) of the models. Further, our study brings out the fact that the continuum field theory corresponding to any discrete model is not unique, even with respect to symmetry considerations, as the choice of field variable is not unique. This leads to ostensible ambiguities, in a manner reminiscent of redundant operators in equilibrium critical phenomena [15].

The plan of the paper is as follows. In Sec. II we define the family of discrete k-hop models and describe certain characteristics of their steady states. In Sec. III we turn to a continuum field-theoretic description of the models, and discuss expectations for asymptotic scaling laws. We also discuss ambiguities in field-theory predictions arising from different definitions of the field variable. In Sec. IV we present the results of our numerical study. Section V is the conclusion.

II. k-HOP MODELS

In this section we introduce a family of models which interpolates between models of interfaces in the low-noise Ising and Toom models in two dimensions.

To begin, consider a square-lattice Ising model evolving in time under single spin-flip Glauber dynamics. In the limit of field and temperature much less than exchange coupling, the allowed configurations of a tilted interface separating up and down phases are directed walks with no overhangs. The time evolution proceeds by corner flips [9], which makes the large-exchange limit of the model identical to the single-step model [10]. Further, there is a one-to-one mapping between directed walk configurations of the interface and configurations of a lattice gas. This is done by identifying a vertical step in the interface with a particle and a horizontal step with a hole. The lattice-gas dynamics involves nearest-neighbor particle-hole exchange, with unequal hopping rates to the right and left—the asymmetric exclusion process. The dynamics of this lattice-gas model has been very well studied: see, for example, [7, 16–18].

The Toom model is a cellular automaton with spins on a square lattice which evolve according to a directional north-east stochastic majority rule [11, 12]. In the low-noise limit the configurations of an interface between up and down spin phases are directed walks, as for the Ising model. However, the evolution rule is different. In terms of the equivalent lattice gas, a particle (hole) exchanges positions with the nearest hole (particle) on the right. This interface model has been analyzed both analytically and numerically [13, 14].

We are now in a position to define the k-hop models. In each of these models, allowed configurations of the interface are directed walks, which, as we have seen above, are equivalent to configurations of a one-dimensional lattice gas. The dynamical evolution rule is most conveniently defined in terms of the lattice gas: first, pick a site at random. If occupied by a particle (hole), exchange it with the nearest hole (particle) on its right with probability p (q), provided that separation of the two sites in question is k lattice spacings or less.

In the first member of the family of models, $k = 1$, only nearest-neighbor particle-hole exchanges are allowed. The resulting lattice-gas dynamics is the asymmetric exclusion process, which, as discussed above, is equivalent to the dynamics of a two-dimensional (2D) Glauber-Ising system in a magnetic field. (The hopping rates p and q involve combinations of the field and temperature [9].) In the other extreme, $k \to \infty$, there is no limit on the length of the hops. Actual hops will of course typically be only of the size of a particle or hole cluster, and therefore a local continuum description is valid. The dynamics is that of a Toom interface in the low-noise limit [13, 14].

Next, we characterize some features of the steady states of k-hop models. The dynamical rule clearly conserves the number of particles, N_P. In the steady state, each microscopic configuration C with N_P particles occurs with equal probability. This can be seen as follows: for each transition away from C with rate p (q), there is a distinct and unique configuration C' which evolves into C at the same rate. The construction of C' is illustrated in Fig. 1. If the transition away from C involves a particle exchanging with a hole a distance l on its right ($l \leq k$), the configuration C' is constructed by exchanging the lth particle in the same particle cluster with the first hole on the left of the cluster. A similar construction can be used for hole hops. The (unnormalized) state $\sum_C |C\rangle$ which weighs all microscopic N_P-particle configurations $|C\rangle$ equally is then the steady state, as the total transition rates in and out of each microscopic configuration $|C\rangle$ are equal.

In the thermodynamic limit $N \to \infty$, $N_P \to \infty$, $N_P/N = \rho$, equal likelihood of all microscopic states is tantamount to product measure. Each site is occupied by a particle with probability ρ, independent of the occupation of particles on all other sites.

As a result, it is a simple matter to calculate the steady state current in the infinite system. The mean distance traveled to the right by a particle is $R = \sum_{r=0}^{k} r\,\mathrm{prob}(r)$, where $\mathrm{prob}(r) = \rho^{r-1}(1-\rho)$ is the probability that the next $(r-1)$ successive sites are occupied by particles, and the rth site by a hole. Similarly, the mean distance traveled by a hole in a hop to the right is $R = \sum_{r=0}^{k} r\rho(1-\rho)^{r-1}$. The current (which has contributions from hops of both particles and holes) is then

$$J_k(\rho) = p(1-\rho)\sum_{r=0}^{k} r\rho^r - q\rho\sum_{r=0}^{k} r(1-\rho)^r. \qquad (2)$$

The geometric series in this equation may be summed, but we prefer to write the current as in (2), to emphasize the fact that $J_k(\rho)$ is a polynomial of order $(k+1)$. In the limit $k \to \infty$, we recover $J_{\mathrm{Toom}} = p\rho/(1-\rho) - q(1-\rho)/\rho$: see, for example, [13].

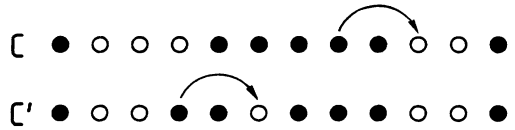

FIG. 1. Construction of a configuration C' from which one can reach a given configuration C by an allowed particle hop of length $\leq k$ with probability p.

The nonlinear dependence of J_k on ρ has an immediate important physical consequence. The system supports kinematic waves [19] which move through the system at speed $U = \partial J_k/\partial\rho$. This velocity is quite different from average particle velocity $v_P = J_k/\rho$. Kinematic waves, whose origin is the conservation of particle number, are parity-breaking waves first discussed in a general way by Lighthill and Whitham [19]. In the context of stochastic lattice gases, the kinematic wave transports the pattern of density fluctuations in the initial state through the system at speed U [9, 20]. For the corresponding interface problem, the motion corresponds to a traveling wave which transports transverse interface fluctuations [9].

As discussed in detail in the next section, the second derivative $j_2 \equiv \partial^2 J_k/\partial\rho^2$ is important in determining the asymptotic scaling law for the correlation function involving density fluctuations in the lattice gas (or height fluctuations in the interface). Here we give the result for later reference:

$$j_2 \equiv \partial^2 J_k/\partial\rho^2 = w_P - w_H, \tag{3}$$

with

$$w_P = \frac{p}{(1-\rho)^3} F_k(\rho),$$
$$w_H = \frac{q}{\rho^3} F_k(1-\rho). \tag{4}$$

The function $F_k(\rho)$ is given by

$$F_k(\rho) = 2 + \rho^{k-1}(c_0 + c_1\rho + c_2\rho^2 + c_3\rho^3), \tag{5}$$

with

$$c_0 = -k(k+1)^2, \quad c_1 = 3k^3 + 5k^2 - 2,$$
$$c_2 = k(1 - 4k - 3k^2), \quad c_3 = k^2(k+1).$$

We close this section by drawing attention to an important consequence of the current $J_k(\rho)$ in Eq. (2) being a polynomial of order $(k+1)$ in ρ. We will see in Sec. III B that this implies that at most the first $(k+1)$ terms in the gradient expansion on the right hand side of Eq. (1) are nonzero. This controllable nonlinearity is a useful feature of k-hop models.

III. FIELD-THEORY DESCRIPTION

A. Scaling properties

The scaling behavior of height or density fluctuations is determined by the coefficients b_m in (1). The constant b_0 specifies the mean rate of growth of the interface. It can be eliminated by redefining the height variable $h \to h + b_0 t$. If b_1 is nonzero, the autocorrelation function grows asymptotically as $S(0,t) \sim t^{1/2}$ [7]. In this case b_1 has a simple physical meaning—it is the speed of kinematic waves which transport fluctuations through the system. As discussed in Sec. II, kinematic waves carry longitudinal density fluctuations through the lattice gas at speed $\partial J_k/\partial\rho$ or, equivalently, transverse fluctuations across the interface. The first-order gradient term can be eliminated from (1) by the Galilean shift $x \to x + b_1 t$, corresponding to using a frame which moves along with the wave. Henceforth we assume that these transformations have been made.

If $b_0 = b_1 = 0$, the autocorrelation function senses the dissipation of the kinematic wave, and $S(x,t)$ assumes the scaling form

$$S(x,t) \sim b t^{\beta} Y\left(\frac{ax}{t^z}\right) \tag{6}$$

in the asymptotic limit $x, t \to \infty$, with $x/t^z = \text{const}$. The critical exponents β and z and the scaling function Y are the same for all systems belonging to the same universality class, while a and b are system-dependent (nonuniversal) metric factors. Different universality classes describe different patterns of decay of the kinematic wave.

A perturbative RG analysis indicates that there are two distinct fixed points, and hence two universality classes. The first class is the one characterized by all $b_m = 0$. In this case, (1) describes a linear growth problem which was studied by Edwards and Wilkinson [6], and in a different context by Hammersley [5]. The corresponding values of z and β are 2 and 1/4, respectively. The Hammersley-Edwards-Wilkinson (HEW) fixed point also controls the behavior of systems with only odd-order b_m with $m \geq 3$. The lowest-order nonlinearity is then cubic, and simple power counting shows that it is marginal at the HEW fixed point. A recent RG calculation shows, in fact, that the nonlinearity is marginally irrelevant [14], and leads to multiplicative logarithmic corrections to the power law for linear growth:

$$S(0,t) \sim t^{1/4} (\ln t)^{1/8}. \tag{7}$$

This result agrees with mode-coupling calculations [21]. The form of (7) has been numerically confirmed for the low-noise Toom interface [14]; additional cases are studied below.

Since they break the $h \to -h$ symmetry, even-order b_m coefficients lead to a change of the universality class. For instance, the second-order nonlinearity b_2 is a relevant perturbation which drives the system from the HEW fixed point to a new (Kardar-Parisi-Zhang, KPZ) fixed point [2, 3] characterized by the exponents $z = 3/2$ and $\beta = 1/3$. It is important to realize that the relevant scaling field which describes the outflow away from the HEW fixed point has components along all even-order b_m, and not only along b_2 as would be suggested by simple power counting. Consequently, even if b_2 vanishes, as long as even one of the coefficients $b_4, b_6, \ldots$ is nonzero, an outflow will be generically triggered. This is in agreement with the findings of the numerical integration of a stochastic differential equation with only a quartic nonlinearity [22]; the result is consistent with KPZ behavior.

Of course, appropriate scaling laws hold only asymptotically. For instance, if b_2 is small, the behavior over substantial regimes of t may appear HEW-like; truly asymptotic KPZ behavior would be expected to set in only over very long times. Further, long crossover times may occur if $b_2 = 0$ but $b_4, b_6, \ldots \neq 0$.

In order to test these theoretical predictions in the models under consideration here, the first task is to iden-

tify the coefficients b_m appropriate to the k-hop models. We now turn to this.

B. Coarse-grained description

The continuum description of the lattice gas (particles and holes moving with discrete jump dynamics) is constructed by coarse graining over regions which are large enough to contain many lattice sites. The coarse-grained density $\rho(x)$ is coupled to the local current $J(x)$ through the continuity equation

$$\frac{\partial \rho}{\partial t} + \frac{\partial J(x)}{\partial x} = 0. \tag{8}$$

We write the current $J(x)$ as

$$J(x) = -\nu \frac{\partial \rho}{\partial x} + j(\rho) + \eta, \tag{9}$$

where ν is the particle diffusion constant, η is a Gaussian noise variable, and $j(\rho)$ is the systematic contribution to the current associated with the local density ρ. In the usual spirit of hydrodynamics [1, 4], we take $j(\rho)$ to be the macroscopic current $J_k(\rho)$ corresponding to density ρ, and expand in a power series in the density fluctuation $\phi \equiv \rho - \bar{\rho}$ around the mean macroscopic density $\bar{\rho} = N_P/N$. Then,

$$j(\rho) = \sum_m j_m \phi^m, \tag{10}$$

with $m! j_m = \partial^m J_k / \partial \rho^m$. Defining a height variable $h(x,t)$ by

$$h(x,t) = \int_{x_0}^{x} \phi(x',t) dx', \tag{11}$$

we see that h satisfies (1), with b_m replaced by j_m. Since we know the current $J_k(\rho)$ explicitly, the derivatives j_m can be found. These quantities specify the "bare" or unrenormalized values of the coefficients b_m. As usual, under RG flow, or equivalently at large length and time scales, the coefficients themselves are renormalized, ultimately approaching their fixed point values. Asymptotic scaling is determined by which basin of attraction the initial unrenormalized values lie within. Let us see what this implies for the k-hop models. Here $j(\rho)$ is identified with the macroscopic current $J_k(\rho)$ calculated in (2), and the derivatives $j_m \equiv b_m$ can be found for each member of the family, in terms of the microscopic parameters k, p, q, and ρ. As $J_k(\rho)$ is a polynomial, only the first $(k+1)$ derivatives are nonzero.

$k = 1$. This is the low-noise Ising interface model, or exclusion process. All b_m with $m \geq 3$ vanish. The second-order coefficient b_2 vanishes along the locus $p = q$, implying that HEW behavior holds on this locus. If $p \neq q$, the second-order coefficients are nonzero, implying KPZ behavior.

$k = 2$. In this case fourth- and higher-order b_m vanish. The condition $b_2 = 0$ defines a locus of points along which the HEW fixed point governs scaling behavior, but b_3 is nonzero, leading to multiplicative logarithmic corrections to the HEW power law. KPZ behavior is expected elsewhere.

$k \geq 3$. Although the condition $b_2 = 0$ may be met along particular loci, this does not imply that HEW behavior occurs. Since higher-even-order b_m are present in general, b_2 is generated at large scales even if its unrenormalized value is zero. All even-order nonlinearities vanish only at the symmetric point $p = q$, $\rho = 1/2$. Hence HEW behavior is expected, with logarithmic corrections, only at this point. Elsewhere, the asymptotic behavior is controlled by the KPZ fixed point.

A numerical study of these predictions is described in Sec. IV.

C. Coarse graining in tag space

A related but different model of an interface is obtained from a one-dimensional lattice gas on viewing the tag (particle label) as a spatial coordinate, and relating the displacement of a particle to interface height [7]. Let us suppose that all particles are labeled sequentially at $t = 0$. When a particle is exchanged with a hole m lattice spacings away, reinterpret the move as each of the m particles in between hopping one unit to the right, rather than as a single long hop of one particle. With this interpretation, the ordering of particles is preserved, which enables particle labels (tags), denoted by n, to be used as coordinates. In the usual fashion, particle labels are coarse grained, so that n becomes continuous.

The connection between the earlier description and the tag-space description is obtained by writing the density as

$$\rho(x,t) = \int \delta(y(n,t) - x) \mathrm{d}n. \tag{12}$$

The quantity $y(n,t)$ is the position of the nth particle at time t. From (11) and (12), it follows that

$$\frac{\partial h}{\partial t} = -\frac{\partial y}{\partial t} \left| \frac{\partial y}{\partial n} \right|^{-1} \Bigg|_{y=x}, \tag{13}$$

$$\frac{\partial h}{\partial x} = \left| \frac{\partial y}{\partial n} \right|^{-1} \Bigg|_{y=x} - \bar{\rho}. \tag{14}$$

Substituting these expressions into (1) as applied to h, a different equation for a new height variable, $\tilde{h} = n - \bar{\rho} y$ is obtained:

$$\frac{\partial \tilde{h}}{\partial t} = \rho^2 \nu \frac{\partial^2 \tilde{h}}{\partial^2 n} + \sum_m a_m \left(\frac{\partial \tilde{h}}{\partial n} \right)^m + \eta(n,t). \tag{15}$$

The coefficients a_m are expressed in terms of the coefficients j_m as follows:

$$\begin{aligned} a_1 &= -j_0/\bar{\rho}, \\ a_2 &= -j_0/\bar{\rho} + j_1, \\ a_3 &= \bar{\rho} j_2 + \bar{\rho}^2 j_3, \\ a_4 &= \bar{\rho} j_2 + 2\bar{\rho}^2 j_3 + \bar{\rho}^3 j_4. \end{aligned} \tag{16}$$

Notice that j_1 is the speed of the kinematic wave with respect to a space-fixed axis, whereas a_1 is the wave speed with respect to a frame moving with the average speed of the particles. The first-order gradient term, $\partial h/\partial x$ or $\partial \tilde{h}/\partial n$, can be eliminated by the appropriate Galilean shift. The second-order terms j_2 and a_2 are proportional to each other and so both terms vanish along the same k-dependent locus in the bias-density plane. However, higher-order terms do not vanish simultaneously in the two descriptions, and they do not have the same symmetry. Even if all the even-order j_m vanish, thus leading to HEW behavior for interface fluctuations in the original variable h, the corresponding even-order a_m for $m \geq 4$ are finite as long as, for example, the cubic term j_3 is finite. This paradoxically suggests that the scaling behavior of fluctuations should be controlled by the KPZ fixed point even when all even-order j_m are zero.

The situation bears an analogy to the occurrence and effects of redundant operators in RG studies of equilibrium critical phenomena. Envisaged as arising from a redefinition of a field variable [15], redundant operators have shown up as important operators in several contexts, such as Monte Carlo RG [23]. However, even when present, they have no effect on physical observables; moreover, the right choice of variables suppresses them altogether. Proceeding by analogy, we argue that the change to a tag-based description has brought into play redundant operators which are spurious. The field theory for the problem is probably best formulated and understood in terms of the interface variables of (11), although the tag description turns out to be better for obtaining numerical results.

IV. NUMERICAL RESULTS

In this section we report numerical measurements which test the theoretical predictions of the preceding section.

First, we describe the method of simulation. An initial condition is generated by distributing the required number of particles N_P randomly on the lattice. Then, one of N_S sites is picked at random; if occupied by a particle (hole), it is exchanged with the closest hole (particle) on the right with probability p (q), provided that the separation of the sites is k units or less. However, we take care to respect the sequential ordering of tags for particles and holes during the exchanges. We have arbitrarily set $p = 1$ to minimize the need to generate random numbers. Since we argued in Sec. II that a product measure exists, the system is at steady state from $t = 0$, and no equilibration time is necessary. Periodic boundary conditions have been used. The term "time step" will be used to indicate N_S exchange attempts, or an average of one attempt to the right per site. Finally, we note that a lever rule has been used to minimize errors when n_t (defined in the next paragraph) is not an integer.

Next we will discuss the relative merits of measuring different types of correlation functions. The first is the height-height correlation function

$$S(0,t) = \langle [h(x'+Ut,t) - h(x',0)]^2 \rangle, \tag{17}$$

where $h(x,t)$ is given by (11), with $x_0 = Ut$, and is calculated with periodic boundary conditions so that $0 \leq h(x,t) \leq N_P$, where N_P is the number of particles. The other is the sliding-tag correlation function [7]

$$\sigma(u,t) = \langle [y_{n_t}(t) - y_n(0) - ut]^2 \rangle, \tag{18}$$

where $n_t = n + \rho(u - v_P)t$ represents the shift of particle label in time t. We have chosen the sliding-tag parameter to be $u = U = \partial j/\partial \rho$ in order to keep up with the moving density pattern. The choice $u = U$ is analogous to the choice of $x_0 = Ut$ in the previous case, and leads to a minimum over all $\sigma(u,t)$.

We performed numerous simulations and measurements of both correlation functions above. The sliding-tag correlation function σ shows much smaller fluctuations than S does, although in the cases where an analytical answer is known the exponents obtained by both methods agree to within statistical error. This is illustrated in Fig. 2, which shows results for a system of size $N_S = 10\,000$ with $k = 2$, $q/p = 1$, $\rho = 1/2$ for the *same* evolution in time, using both types of correlation function. The total time of the simulation is 4000 Monte Carlo (MC) steps/site and the sampling interval is ten time steps. In both cases the long-time behavior is consistent with $\sigma \sim t^{1/4}$, in agreement with analytical predictions for the symmetric point (see Sec. III A). The reason for the difference in the level of fluctuations is not clear to us; a possibility is the fact that in (11), $h(x,t)$ is defined with respect to an origin x_0, which moves at the average speed, rather than at the actual fluctuating speed of the density wave. The correlation function $S(0,t)$ can then be quite sensitive to this origin. We attempted to improve the statistics by using several equally spaced origins, and averaging the results. This resulted in a considerable decrease in the level of fast oscillations, but the results for up to five origins were still not nearly as smooth as for $\sigma(u,t)$. Henceforth all simulations refer to the correlation function $\sigma(u,t)$; relevant plots, unless otherwise indicated, show the square of this quantity.

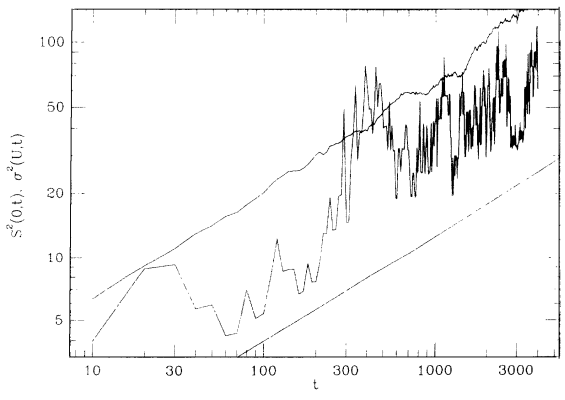

FIG. 2. Comparison of $S^2(0,t)$ (middle, noisy curve) and $\sigma^2(U,t)$ (upper, less noisy curve) for a common Monte Carlo history: $k = 2$, $p/q = 1$, 10 000 sites, and 4000 time steps, sampled every ten steps. Both curves are consistent with the predicted $t^{1/2}$ behavior (lower, straight line), but there is a marked difference in the level of noise.

Before presenting numerical results, it should prove instructive to see what the $j_2 = 0$ loci look like for different values of k; the general expression was presented in (3)–(5). As is usual in these cases, we concentrate on the region $\rho \leq 1/2$, $0 \leq (q/p) \leq 1$, shown in Fig. 3. For $k = 1$, the entire $(q/p) = 1$ line corresponds to the locus. The other natural limit is the Toom model ($k = \infty$), also shown in the figure. One should notice that for $k < \infty$ the loci do not approach the Toom limit, $(q/p) = [\rho/(1-\rho)]^3$, in a monotonic fashion. In fact, for k between 5 and 7, no points of the locus are present in this region. This is caused by a singularity in (3)–(5), which makes some of the values of (q/p) for the loci be greater than 1 in the range of ρ under consideration. The explicit parameter values studied numerically below are indicated in the figure with circles ($j_2 = 0$), or squares ($j_2 \neq 0$).

$k = 1$, $j_2 = 0$. We consider in the first instance the case $k = 1$, for which all higher-order b_m coefficients are zero along the $j_2 = 0$ locus, which in this case corresponds to the entire line $q/p = 1$. On this line, we have chosen the value $\rho = 1/4$. Figure 4 shows σ^2 divided by $t^{1/2}$ (top) and $t^{1/2}(\ln t)^{1/4}$ (bottom) respectively, for the average of five independent runs of 300 000 sites each, simulated for 160 000 time steps (x axis). For purposes of comparison, the quantities plotted, times, and system sizes in Fig. 5 will be the same. In this case the correlation function seems to follow the predicted HEW scaling law, as the data in the top half are more or less horizontal, while those in the bottom decrease. No logarithmic corrections to the scaling law seem to be present.

$k = 2$, $j_2 = 0$. In contrast with the previous case, Fig. 5 here shows multiplicative logarithmic corrections to HEW behavior. In this case $j_3 \neq 0$, but all higher-order $j_m = 0$. We stress that, unlike for higher values of k, the entire locus $j_2 = 0$ is critical in this case (for $k \geq 3$, only the symmetric point shows $\sigma \sim t^{1/4}$ behavior, with logarithmic corrections).

$k = 2$, $j_2 \neq 0$. We now show what happens away from the $j_2 = 0$ locus; we consider the case $k = 2$, $p = q = 1$, $\rho = 2/5$. In this case, crossover to KPZ

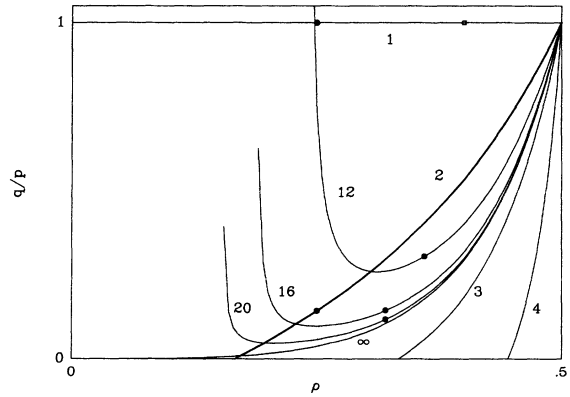

FIG. 3. Loci along which $j_2 = 0$ for various values of hopping cutoff k, in the q/p vs ρ plane. For some values of k (5, 6, 7) no points of the locus lie in the region shown. Notice the nonmonotonic approach to the Toom limit. We have marked particular parameter values used in subsequent figures. Circles: $j_2 = 0$ locus. Squares: $j_2 \neq 0$.

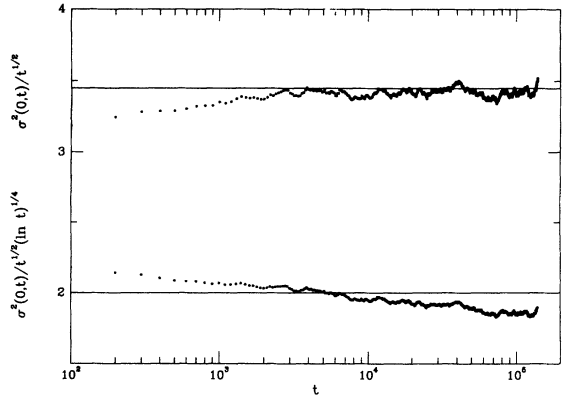

FIG. 4. Correlation function σ^2 divided by $t^{1/2}$ (upper half), and by $t^{1/2}(\ln t)^{1/4}$ (lower half) for $k = 1$ along the $(q/p) = 1$ line. The average over five independent simulations on a system of 300 000 sites is shown. This model is evidently in the HEW universality class. No logarithmic corrections are apparent.

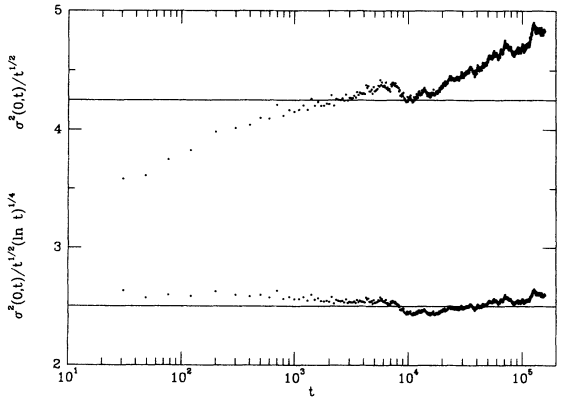

FIG. 5. Same quantities as in the previous figure, but for $k = 2$, $q/p = 1/7$. Same times and number of realizations as in the previous figure. The existence of logarithmic corrections to the usual HEW power law behavior is apparent.

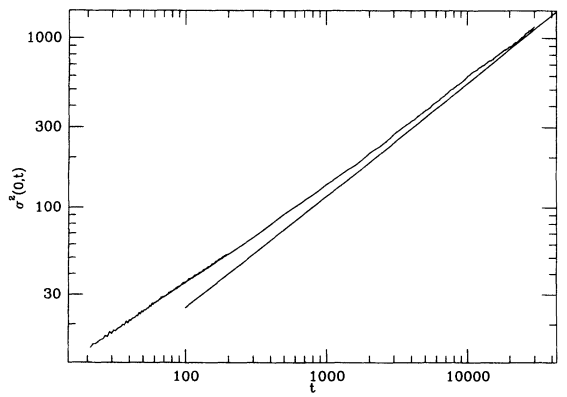

FIG. 6. Correlation function σ^2 vs time for $k = 2$, $\rho = 2/5$, $q/p = 1$. Crossover to KPZ behavior is apparent after 3000–4000 time steps (the lower straight line has slope 2/3). Each point is the average over five independent simulations on a system of 300 000 sites.

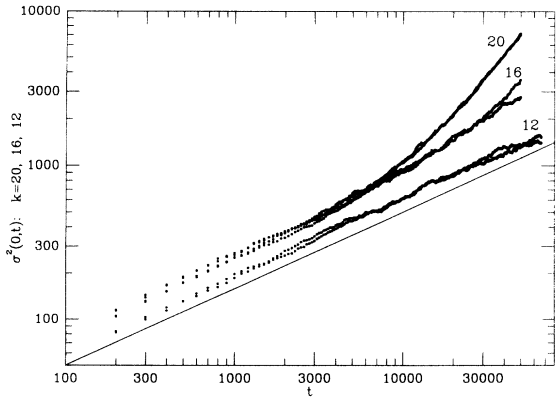

FIG. 7. Crossover away from HEW behavior for large values of k along the locus $j_2 = 0$. Two independent runs (300 000 sites each) are shown for $k = 20$ (upper curves), $k = 16$ (middle curves), and $k = 12$ (lower curves). Deviations from HEW behavior (the lower line has slope 1/2) are apparent before 70 000 time steps for $k = 20$ and $k = 16$, but not for $k = 12$.

behavior is predicted, but some HEW-like behavior may be apparent for short times, as the parameters are not too far away from the HEW locus. This is seen clearly in Fig. 6, which shows a logarithmic plot of σ^2 vs time. The curve (averaged over five configurations of 300 000 sites each) approaches a line with slope 2/3 (asymptotic KPZ behavior) only after 3000–4000 time steps. Moving further away from the critical line results in earlier onset of KPZ behavior.

$k > 2$. The final point of the numerical results is to illustrate deviations from HEW behavior *along* the $j_2 = 0$ locus for larger k: if $k \geq 3$, there will be in general nonzero coefficients up to j_{k+1}. Generically, the even-order coefficients have a component along the scaling axis, resulting in a prediction of crossover away from the HEW fixed point. We see evidence of such a crossover for $k \geq 16$ (Fig. 7), although the asymptotic behavior has not been reached over the times considered. Figure 7 suggests that the crossover times become longer as k decreases; in fact, we have been unable to see the crossover for $k = 12$ over times $t \leq 70\,000$. For large but finite k, the locus $j_2 = 0$ shows a minimum as a function of ρ in the region considered; exploration for $k = 16$ did not show any evidence of change from $\sigma \sim t^{1/4}$ behavior to the left of the minimum, over the times considered.

V. SUMMARY AND DISCUSSION

The models of asymmetrically hopping particles that we have studied in this paper share an important property—they all have a simple steady state which is characterized by product measure in the infinite system. This feature leads to the explicit computability of the unrenormalized b_m coefficients in the hydrodynamic theory, and this in turn enables comparison with RG predictions.

Another family of models, which also includes the $k = 1$ Ising interface model as a limit, has been studied recently by Devillard and Spohn [21]. Their study confirms that a cubic nonlinearity is marginally irrelevant at the HEW fixed point. The present study goes one step further in providing a numerical verification of the form of multiplicative logarithmic corrections predicted by RG [14] and mode-coupling theory [21]. Monitoring fluctuations using the tag description rather than a real-space formulation has been useful in obtaining meaningful numerical results.

The HEW fixed point controls the asymptotic behavior of correlation functions if all even-order b_m are absent. This condition is satisfied only at special points, or along exceptional loci, in the bias-density plane. For $k = 1$, the locus is the line $p = q$, which, for the Ising model interface (to which this model is equivalent), corresponds to the condition of zero field. In this case, odd-order b_m vanish as well, so that asymptotically $\sigma \sim t^{1/4}$ holds. Turning to the $k = 2$ model, once again even-order b_m vanish along a special locus — but this time b_3 is nonzero, and is expected to induce multiplicative logarithmic corrections to the pure HEW power law. Figures 4 and 5 provide clear evidence for the absence of multiplicative logarithmic corrections in the $k = 1$ model, and their presence in the $k = 2$ model. For models with $k \geq 3$, even-order b_m vanish only at the single point $p = q$, $\rho = 1/2$, so that HEW behavior (with multiplicative logarithms) is expected only at this symmetric point, a feature that was found in an earlier study of the Toom ($k = \infty$) model [14].

At all other points of the phase diagrams of the k-hop models, even-order b_m are nonzero. Generically, this would imply that the HEW fixed point is unstable; recall that the scaling field describing this outflow has components along all even-order b_m, so that if, for example, the condition $b_2 = 0$, $b_4 \neq 0$ is met, the asymptotic behavior should deviate from HEW expectations. A recent integration of a stochastic differential equation with a quartic nonlinearity by Amar and Family [22] bears this out. In the present work, we have numerical confirmation of these ideas for large k (≥ 16) models (Fig. 7). The results also show that the crossover time needed for the asymptotic behavior to set in depends on k, and seems to be larger than the time of observation for the smaller k (≤ 12) models.

A final point that our study touches on is the apparent ambiguity in the stability of the HEW fixed point, based on two different field-theoretic descriptions of the same lattice-gas models. We conjecture that the difference arises from the analogs of redundant operators in this problem. This seems like an interesting question, deserving further study.

ACKNOWLEDGMENTS

P.B. and M.P. thank the Physics Department at the University of Oxford for its hospitality; M.B. acknowledges the hospitality of the Condensed Matter group at ICTP, Trieste. The work of P.B. and M.B. at Oxford was supported by the Science and Engineering Research Council (UK); the work of M.P. was supported by the U.S. Department of Energy Division of Materials Science, under Contract No. DE-AC02-76CH00016. We thank R. B. Stinchcombe for useful discussions, and S. N. Majumdar for helpful correspondence.

[1] J. L. Lebowitz, E. Presutti, and H. Spohn, J. Stat. Phys. **51**, 841 (1988).
[2] M. Kardar, G. Parisi, and Y. Zhang, Phys. Rev. Lett. **56**, 889 (1986).
[3] E. Medina, T. Hwa, M. Kardar, and Y. Zhang, Phys. Rev. A **39**, 3053 (1989).
[4] H. van Beijeren, R. Kutner, and H. Spohn, Phys. Rev. Lett. **54**, 2026 (1985).
[5] J. M. Hammersley, in *Proceedings of the Fifth Berkeley Symposium on Mathematical Statistics and Probability*, edited by L. M. Le Cam and J. Neyman (University of California Press, Berkeley, 1967).
[6] S. F. Edwards and D. R. Wilkinson, Proc. R. Soc. London, Ser. A **381**, 17 (1982).
[7] S. N. Majumdar and M. Barma, Phys. Rev. B **44**, 5306 (1991); Physica A **177**, 366 (1991).
[8] J. Krug and H. Spohn, in *Solids far from Equilibrium*, edited by C. Godreche (Cambridge University Press, Cambridge, England, 1992).
[9] M. Barma, J. Phys. A **25**, L693 (1992).
[10] P. Meakin, P. Ramanlal, L. M. Sander, and R. C. Ball, Phys. Rev. A **34**, 5091 (1986).
[11] A. L. Toom, in *Multicomponent Random Systems*, edited by R. L. Dobrushin and Ya. G. Sinai (Marcel Dekker, New York, 1980).
[12] C. H. Bennett and G. Grinstein, Phys. Rev. Lett. **55**, 657 (1985).
[13] B. Derrida, J. L. Lebowitz, E. R. Speer, and H. Spohn, Phys. Rev. Lett. **67**, 165 (1991); J. Phys. A **24**, 4805 (1991).
[14] M. Paczuski, M. Barma, S. N. Majumdar, and T. Hwa, Phys. Rev. Lett. **69**, 2735 (1992).
[15] Recall that a redundant operator is an unphysical entity typically generated by a change of the field variable: see F. J. Wegner, J. Phys. C **7**, 2098 (1974).
[16] T. M. Liggett, *Interacting Particle Systems* (Springer, New York, 1985).
[17] P. A. Ferrari, Ann. Inst. Henri Poincare **55**, 637 (1991).
[18] L.-H. Gwa and H. Spohn, Phys. Rev. Lett. **68**, 725 (1992).
[19] M. J. Lighthill and G. B. Whitham, Proc. R. Soc. London, Ser. A **229**, 281 (1955); **229**, 317 (1955).
[20] H. van Beijeren, J. Stat. Phys. **63**, 47 (1991).
[21] P. Devillard and H. Spohn, J. Stat. Phys. **66**, 1089 (1992).
[22] J. G. Amar and F. Family, Phys. Rev. E **47**, 1595 (1993).
[23] G. S. Pawley, R. H. Swendsen, D. J. Wallace, and K. G. Wilson, Phys. Rev. B **29**, 4030 (1984); G. Murthy and R. Shankar, *ibid.* **32**, 5851 (1985); R. Shankar and R. Gupta, *ibid.* **32**, 6084 (1985).